===== **OPTICAL WAVES PROPAGATION** =====

# Localized High-Intensity Light Structures during Multiple Filamentation of Ti:Sapphire-Laser Femtosecond Pulses along an Air Path

**D. V. Apeksimov[a], \*, A. A. Zemlyanov[a], \*\*, A. N. Iglakova[a], A. M. Kabanov[a], O. I. Kuchinskaya[a, b],**
**G. G. Matvienko[a, b], V. K. Oshlakov[a], A. V. Petrov[a], and E. B. Sokolova[a]**

[a]*V.E. Zuev Institute of Atmospheric Optics, Siberian Branch, Russian Academy of Sciences, Tomsk, 634055 Russia*
[b]*Tomsk State University, Tomsk, 634050 Russia*
*\*e-mail: apeximov@iao.ru*
*\*\*e-mail: zaa@iao.ru*
Received June 27, 2017

**Abstract**—The results of experimental studies of the transverse structure of a laser beam after multiple filamentation are presented. A ring structure of radiation is formed around individual filaments in a beam cross section inside the multiple filamentation domain, and at a dozen meters from it a common ring structure starts forming surrounding postfilamentation light channels (PFC). It is shown that the spectra of the PFC, rings, and beam are significantly different. The ring spectrum broadens asymmetrically relative to the carrier wavelength and is mainly concentrated in the short wavelength region. The PFC spectrum has a significant and more symmetrical broadening and covers the range 630−1000 nm.

Propagation of ultrashort laser radiation after attainment of the critical pulse power $P_{cr}$ is accompanied by its self-focusing and filamentation [1, 2], with strong changes in the energy, spatial, spectral, and angular parameters of the laser radiation. The radiation energy is localized in narrow filaments; its spectral composition significantly enriched. These properties are very important for problems of atmospheric optics: laser sounding of the atmosphere and transport of localized light energy through the atmosphere. To solve them, the filamentation domain should be formed at significant distances from a source, and multiple beam filamentation seems the most appropriate for this.

Localized plasma channels originate during multiple filamentation of high-power femtosecond laser pulses. After the plasma formation ceases, these channels intensively transform into narrow weakly diverging light beams. According to experiments [3], such non-ionized light channels were observed in the atmosphere at distances greater than 1 km. The use of light channels, which are much longer than the filamentation domain, requires a thorough study of their energy, spectral, and spatial properties, and physical nature of their formation.

It has been shown in [4–7] that the angular divergence of postfilamentation channels (PFCs) is only tens of microradians during filamentation of collimated beams, and the radiation spectrum covers the region 400−1100 nm. The angular divergence of PFCs of initially strongly focused beams is higher that of collimated beams and is equal to hundreds of microradians; it first decreases with an increase in the initial pulse power and then saturates at a level of about 500 μrad at $P \sim 100 P_{cr}$ ($P_{cr} = 3.2$ GW in air at the wavelength under study $\lambda = 800$ nm). The mean intensities in PFCs measured in [4, 7] are $10^{11}-10^{12}$ W/cm$^2$.

A ring structure of radiation around PFCs has been revealed for focused [6−9] and collimated beams [10, 11] at a carrier wavelength. Concentric rings observed in [11] surround not individual PFCs, but the entire packet of PFCs during multiple filamentation of the beam. The formation of the ring structure in [6] is connected with the diffraction of pulse radiation in plasma channels formed during the filamentation. In [9], the appearance of the rings is explained by phase and intensity inhomogeneities in a beam cross section under the action of Kerr nonlinearity. A model where a ring structure around PFCs results from the interference of a plasma-defocused wave and a wave from the beam periphery has been suggested in [11].

Thus, the studies of PFCs in [4–11] have shown their characteristic properties, i.e., wide spectrum and
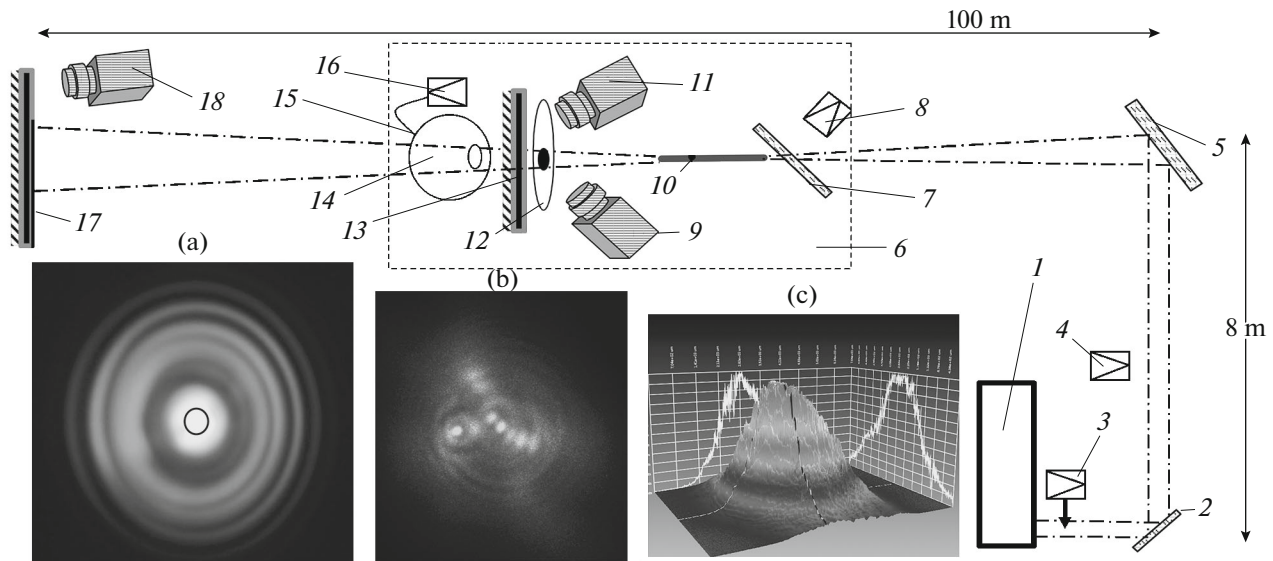
**Fig. 1.** Experimental layout: Ti:Sapphire laser complex (*1*) (*t* = 50 fs, pulse energy *E* = 30 mJ, pulse frequency is 10 Hz, initial beam diameter $d_0$ = 2.5 cm), rotary mirrors (*2* and *5*), pulse energy meter OPHIR-II (*3*), autocorrelator (*4*), movable optical table Thorlabs (*6*), optical wedge OptoSigma WSSQ-50C10-20-3 (*7*), beam energy density profiler LBP2-HR-VIS (*8*), ANDOR-Clara E CCD array (*9*); filamentation domain (*10*), SONY DSC-F828 camera (*11*); diaphragm (*12*), screen (*13*); Newport 819C-SF-6 integrating sphere (*14*), light guide (*15*), Maya2000Pro spectrometer (*16*), fixed screen at the path end (*17*), Pentax K-3 camera (25 Mp) with Pentax100MacroWR macrolens (*18*). (a) Polychrome rings of conical emission recorded on screen *17* (light round in the black circle is the imaging region (b)); (b) beam profile on screen *13*; (c) initial laser beam profile (profiler *8*).

high intensity, maintained at great distances due to small spatial divergence. The questions about formation of the concentric ring structure around individual filaments and a packet of filaments during multiple beam filamentation and about the spectral composition of different components of the postfilamentation structure of a laser beam have not been solved yet.

This work describes the results of experimental studies of the evolution of spatial and spectral structures of a beam during its filamentation. The experimental layout is shown in Fig. 1. The small-scale structure of the beam was recorded by camera *9* on screen *13* with an exposure of 100 ms, which allowed observation of the results of screen illumination by one pulse. An optical table moved along the radiation path, which allowed beam radiation recording during its self-focusing and filamentation. The distance to the beginning of the filamentation domain was 30 m from the path end, i.e., 100 m from the source at an initial radiation energy of 30 mJ. The measurements of the initial beam profile (Fig. 1a) were carried out at the beginning of the path, after rotary mirror *5*; the PFC and ring spectra were measured by spectrometer *16*. A component under study (PFC, ring, and beam) was distinguished using diaphragm *12* mounted before screen *13*, where the beam structure was imaged (see, e.g., Fig. 1b), then screen *13* was taken away, and the radiation was guided into integrating sphere *14*. The accumulation time in spectrometer *16* was 100 ms.

Figure 2 shows an example of transformation of recorded images of the transverse structure of laser beam energy density distribution at a distance of 110 m from the source. The length of the multiple filamentation domain (MFD) detected by burns on light-sensitive paper was 15−20 m. The images show bright spots in the central part of the beam, which are PFCs surrounded by concentric rings of lower brightness, with the intensity decreasing from the beam center toward the periphery. Let us note that the presence and the concentricity of the rings do not depend on the quantity and configuration of filaments in a cross section of MFD and PFCs.

Figure 3a shows the envelope of the energy density of a PFC, which is well approximated by the Gaussian distribution. This fact agrees with the results [12], where a parallelepiped made of K8 glass was placed inside a beam with PFCs, and the filamentation domain was formed inside the glass in the shape of a hollow cone; in accordance with [10], the mean pulse intensity was $10^{11}-10^{12}$ W/cm$^2$. The transverse energy density profile of the PFC along with rings (Fig. 3b) corresponds to the energy density distribution in a Bessel−Gaussian beam. This might well be a cause of abnormally weak ($\sim 10^{-5}$ rad [10]) divergence of PFC (the central part of the resulted distribution). The ring brightness decreases by about two times when moving away from the PFC axis, which agrees well with the ratio of the brightness of interference max-
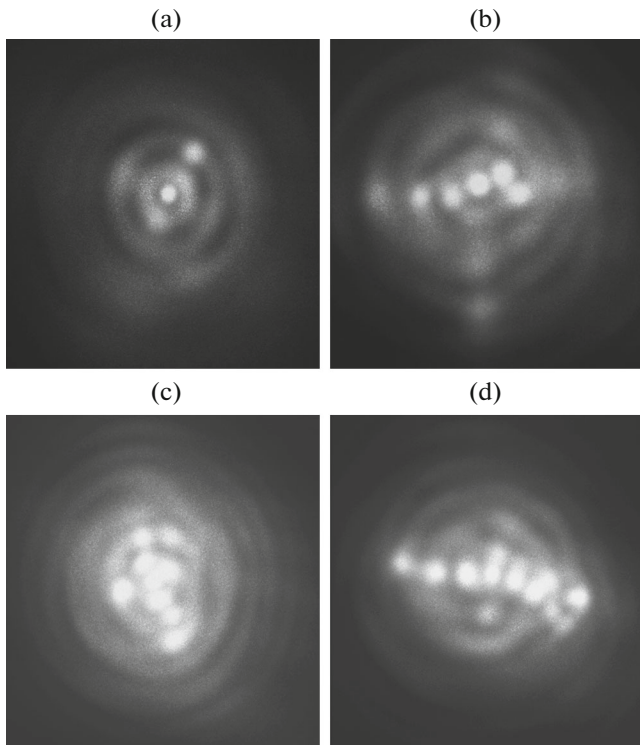
**Fig. 2.** Laser beam transverse structure at a distance of 100 m from the source for a laser pulse with (a) $E = 20$, (b) 23, (c) 27, and (d) 30 mJ.



**Fig. 3.** Envelope of the energy density of (a) an individual PFC and (b) PFC surrounded by a ring system retrieved by the photometry of the image in Fig. 2a using the software for the analysis of laser beam transverse profiles [14].

ima of different orders during light diffraction at a thin obstacle [13].

Let us now consider the origin and evolution of a ring structure at a carrier wavelength. Figure 4 shows the images of the beam structure on screen *13* recorded at different distances from the source. Only bright points are recorded in the beginning of the filamentation domain, which correspond to the channels around filaments with increased energy density (Fig. 4a). In the second half of the filamentation domain, rings appear around them, which surround each filament by the end of the filamentation domain (Figs. 4b and 4c). After the domain (Fig. 4d), these rings transform into the common ring structure. The pattern observed corresponds to the interference of waves from different closely-spaced sources—filaments in our case. It should be also noted that the lateral size of the bright points inside the filamentation domain (~mm) is comparable with the PFC diameter, i.e., it is tens of times larger than the filament diameter. This means that a high-intensity PFC is formed in the beam around each filament, not after the termination of the filamentation region, but at its very beginning, and surrounds each filament.

To refine the physical cause of ring formation, let us consider the results of spectral measurements of different components of the transverse structure of a beam after its filamentation. Figure 5 shows the mea-
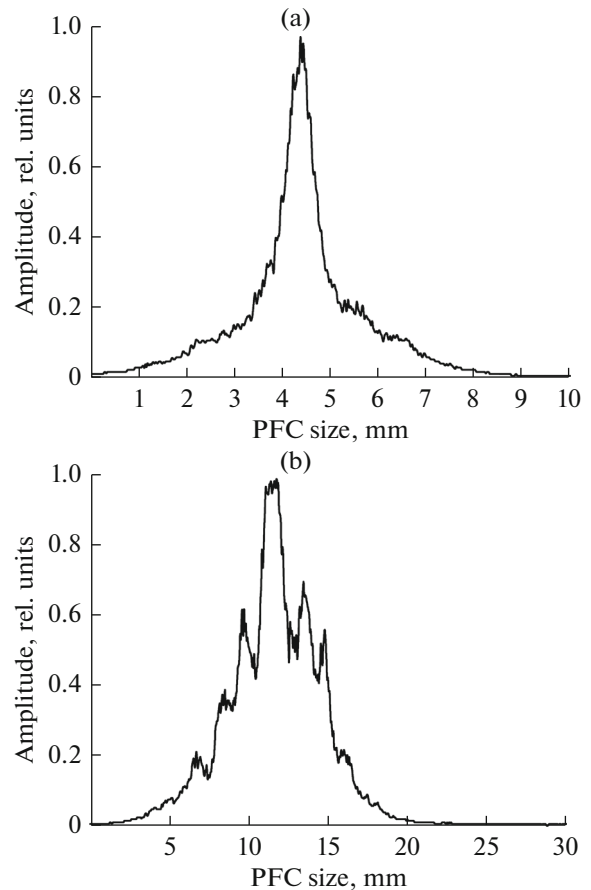
sured spectra of an initial pulse, of a PFC, of a ring around a PFC packet, and of the beam as a whole (except for conical emission rings) at 14 m from the MFD. The spectra are obviously very different. The PFC spectrum broadens into the long- and short-wavelength regions with respect to the carrier wavelength, covers the range 630−1000 nm, and includes quasi-periodic peaks. This behavior of the spectrum points to its formation due to self-induced modulation of the radiation wave phase in a Kerr medium. The spectrum of rings around individual PFCs and the PFC packet broadens asymmetrically and includes only the short-wave component. This broadening (the so-called blue shift) points to either an effect of plasma nonlinearity [15] or the fact that the ring structure is formed only by the pulse tail, because the trailing edge becomes steeper due to the intensity dependence of the group speed [16]. The spectrum of the beam as a whole (out of the rings and PFCs) insignificantly differs from the spectrum of the initial beam.

The measurements of the PFC and ring spectra through diaphragms of the same diameter have shown
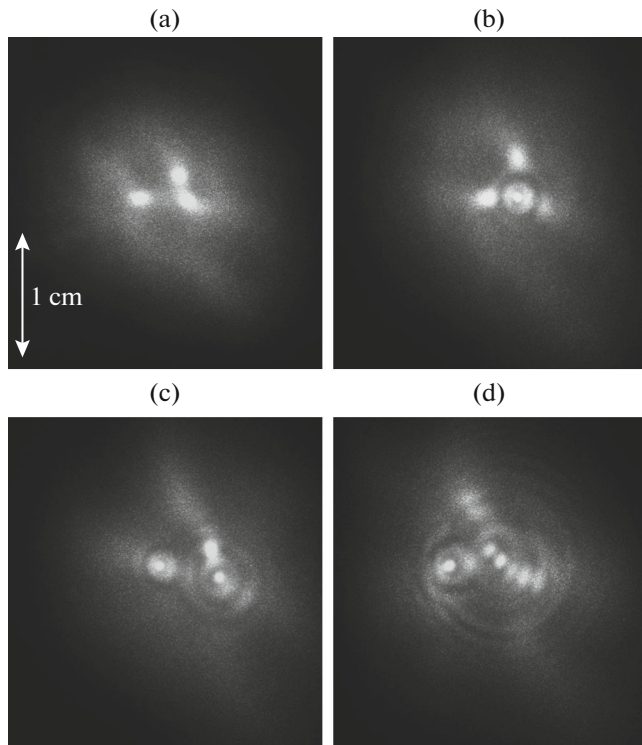
(a)    (b)

1 cm

(c)    (d)

**Fig. 4.** Laser beam transverse structure at a distance of (a) 30, (b) 40, (c) 48, and (d) 57 m from the source; MFD starts at 30 m and ceases at 45 m from the source.
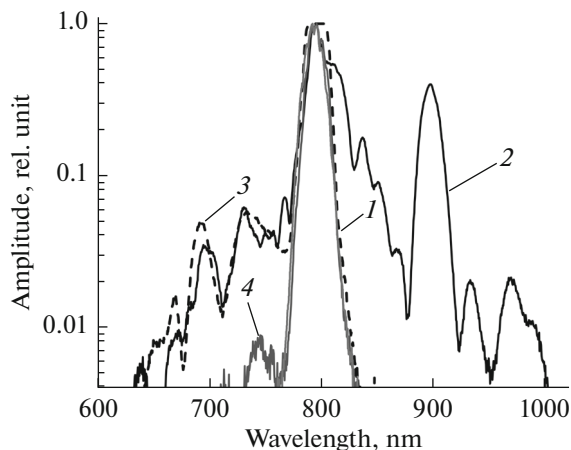


**Fig. 5.** Spectra of the laser beam components at a distance of 14 m from MFD: of initial pulse with $E = 30$ mJ (*1*), of PFC (*2*), of rings (*3*), of the beam out of the MFD and rings (*4*).

that the energy density in a ring the nearest to PFC is approximately half that in the PFC. These results agree well with values shown in Fig. 3b. The PFC area at the measurement point is ~0.1 of the ring area, i.e., the radiation energy in the nearest ring is about five times higher than in the channel. The energy density in the rings significantly decreases moving away from

the MFD. The energy density in PFCs is maintained at great distances due to their weak spatial divergence.

Thus, the results of experimental studies of spatial and spectral transformations of the radiation after the filamentation domain along controllable paths for collimated (focused) beams have shown that the spectra of PFC, rings, and the beam differ. The PFC spectrum significantly and symmetrically broadens and covers the range 630−1000 nm. The broadening of spectrum of rings is asymmetrical and directed mainly to the short wavelength region. These broadenings do not change when moving away from the MFD. The ring structures in a beam cross section are formed around individual filaments inside the MFD; they transform into a common ring structure around PFCs at a distance of tens of meters from the MFD.

## REFERENCES

1. *Self-Focusing: Past and Present. Fundamentals and Prospects*, Ed. by R.W. Boyd, S.G. Lukishova, and Y.R. Shen (Springer, Berlin, 2009), p. 3−19.

2. Yu. E. Geints, A. A. Zemlyanov, A. M. Kabanov, and G. G. Matvienko, *Nonlinear Femtosecond Atmospheric Optics,* Ed. by A.A. Zemlyanov (Publishing House of IAO SB RAS, Tomsk, 2010) [in Russian]

3. G. Mehain, A. Couairon, Y.-B. Andre, C. D' Amico, M. Franco, B. Prade, S. Tzortzakis, A. Mysyrowicz, and R. Sauerbrey, "Long-range self-channeling of infrared laser pulses in air: A new propagation regime without ionization," Appl. Phys. B **79**, 379−382 (2004).

4. Hui Gao, Weiwei Liu, and See Leang Chin, "Post-filamentation multiple light channel formation in air," Laser Phys. **24**, 055301−055308 (2014). doi 10.1088/1054-660X/24/5/055301

5. J.-F. Daigle, O. Kosareva, N. Panov, T.-J. Wang, S. Hosseini, S. Yuan, G. Roy, and S. L. Chin, "Formation and evolution of intense, post-filamentation, ionization-free low divergence beams," Opt. Commun. **284**, 3601−3606 (2011).

6. Yu. E. Geints, A. A. Zemlyanov, A. M. Kabanov, G. G. Matvienko, and A. N. Stepanov, "Self-action of tightly focused femtosecond laser radiation in air in a filamentation regime: Laboratory and numerical experiments," Atmos. Ocean. Opt. **22** (2), 150−157 (2009).

7. D. V. Apeksimov, A. A. Zemlyanov, A. M. Kabanov, and A. N. Stepanov, "Post-filamentation light channels in air," Atmos. Ocean. Opt. **30** (5), 451−455 (2017).

8. N. G. Ivanov and V. F. Losev, "Kerr nonlinearity effect on femtosecond pulse radiation filamentation in air," Atmos. Ocean. Opt. **30** (4), 331−336 (2017).

9. Yu. E. Geints, A. A. Zemlyanov, A. A. Ionin, D. V. Mokrousova, L. V. Seleznev, and E. S. Sunchugasheva,

"Parameters of intense light channels during the post-filamentation stage of ultrashort laser radiation evolution," Atmos. Ocean. Opt. **30** (3), 217−221 (2017).

10. D. V. Apeksimov, A. A. Zemlyanov, A. N. Iglakova, A. M. Kabanov, O. I. Kuchinskaya, G. G. Matvienko, V. K. Oshlakov, and A. V. Petrov, "Postfilamentation channels of terawatt pulses Ti:sapphire-laser in distribution on 150-meter track," Proc. SPIE **10035**, CID: 1003 2M [10035−251] (2016).

11. S. L. Chin, S. Petit, W. Liu, A. Iwasaki, M.-C. Nadeu, V. P. Kandidov, O. G. Kosareva, and K. Yu. Andrianov, "Interference of transverse rings in multifilamentation of powerful femtosecond laser pulses in air," Opt. Commun. **210**, 329 (2002).

12. D. V. Apeksimov, S. S. Golik, A. A. Zemlyanov, A. N. Iglakova, A. M. Kabanov, O. I. Kuchinskaya, G. G. Matvienko, V. K. Oshlakov, A. V. Petrov, and E. B. Sokolova, "Multiple filamentation of collimated laser radiation in water and glass," Atmos. Ocean. Opt. **29** (2), 135−140 (2016).

13. M. Born and E. Wolf, *Principles of Optics* (Pergamon Press, 1970), 4th ed.

14. Yu. E. Geints, D. V. Apeksimov, and A. V. Afonasenko, RF Certificate of Registration of Computer Program No. 2014616871 (June 7, 2014).

15. N. Akozbek, M. Scalora, C. Bowden, and S. L. Chin, "White-light continuum generation and filamentation during the propagation of ultra-short laser pulses in air," Opt. Communs. **191**, 353−362 (2001).

16. S. A. Akhmanov, A. P. Sukhorukov, and R. V. Khokhlov, "Self-focusing and diffraction of light in a nonlinear medium," Phys.-Uspekhi **10**, 609−636 (1968).

*Translated by O. Ponomareva*